

Manuscript Number: ALGAL-D-15-00210R2

Title: New mechanistic model to simulate microalgae growth

Article Type: Full Length Article

Section/Category: Algal Biotechnology

Keywords: Photobioreactors, HRAPS, Photolimitation, Oxygen inhibition, Irradiance, Photosynthetic factories.

Corresponding Author: Prof. Joan Garcia, PhD

Corresponding Author's Institution: Technical University of Catalonia

First Author: Alessandro Solimeno

Order of Authors: Alessandro Solimeno; Roger Samsó; Enrica Uggetti; Bruno Sialve; Jean-Philippe Steyer; Adrián Gabarró; Joan Garcia, PhD

Abstract: The prospect of treating wastewater and at the same time producing microalgae biomass is receiving increasing attention. Mechanistic models for microalgae growth in wastewater are currently being developed for new systems design as well as to improve the understanding of the involved biokinetic processes. However, mathematical models able to describe the complexity of microalgal cultures are still not a common practice. The aim of the present study is to present and calibrate a new mechanistic model built in COMSOL Multiphysics™ platform for the description of microalgae growth. Carbon-limited algal growth, transfer of gases to the atmosphere; and photorespiration, photosynthesis kinetics and photoinhibition are included. The model considers the growth of microalgae as a function of light intensity and temperature, as well as availability of nitrogen and other nutrients. The model was calibrated using experimental data from a case study based on the cultivation of microalgae species in synthetic culture medium. The model was able to reproduce experimental data. Simulations results show the potential of the model to predict microalgae growth and production, nutrient uptake, and the influence of temperature, light intensity and pH on biokinetic processes of microalgae.

# 1                    **New mechanistic model to simulate microalgae growth**

2                    Alessandro Solimeno\*, Roger Samsó\*, Enrica Uggetti\*, Bruno Sialve\*\*, Jean-Philippe  
3                    Steyer\*\*, Adrián Gabarró\* and Joan García\*

4                    \*GEMMA – Group of Environmental Engineering and Microbiology, Department of Hydraulic, Maritime and Environmental  
5                    Engineering, Universitat Politècnica de Catalunya-BarcelonaTech, c/Jordi Girona, 1-3, Building D1, E-08034, Barcelona, Spain.

6                    \*\*INRA, UR0050, Laboratoire de Biotechnologie de l'Environnement, Avenue des Etangs, Narbonne, F-11100, France.

7                    Corresponding author. Tel.: +34 93 401 6464; fax 34 93 401 73 57.

8                    *E-mail address:* joan.garcia@upc.edu (J. García).

## 10                   **Abstract**

11                    The prospect of treating wastewater and at the same time producing microalgae biomass  
12                    is receiving increasing attention. Mechanistic models for microalgae growth in wastewater are  
13                    currently being developed for new systems design as well as to improve the understanding of  
14                    the involved biokinetic processes. However, mathematical models able to describe the  
15                    complexity of microalgal cultures are still not a common practice. The aim of the present study  
16                    is to present and calibrate a new mechanistic model built in COMSOL Multiphysics™  
17                    platform for the description of microalgae growth. Carbon-limited algal growth, transfer of gases  
18                    to the atmosphere; and photorespiration, photosynthesis kinetics and photoinhibition are included.  
19                    The model considers the growth of microalgae as a function of light intensity and temperature,  
20                    as well as availability of nitrogen and other nutrients. The model was calibrated using  
21                    experimental data from a case study based on the cultivation of microalgae species in  
22                    synthetic culture medium. The model was able to reproduce experimental data. Simulations  
23                    results show the potential of the model to predict microalgae growth and production, nutrient  
24                    uptake, and the influence of temperature, light intensity and pH on biokinetic processes of  
25                    microalgae.

26                    **Keywords:** Photobioreactors, HRAPs, Photolimitation, Oxygen inhibition, Irradiance,  
27                    Photosynthetic factories.

## 28                   **1. Introduction**

29                    Microalgae are nowadays used to produce a variety of compounds of interest for  
30                    different industrial sectors such as aquaculture and animal feed, human nutrition,  
31                    cosmetics and nutraceuticals as well as pharmaceuticals (Spolaore et al., 2006; Acién et al.,  
32                    2013). In addition, these microorganisms have a great potential for CO<sub>2</sub> capture and  
33                    biofuels production such as biodiesel (Craggs et al., 2011). In fact, in recent years a  
34                    tremendous effort has been made in numerous research centres to obtain biodiesel from  
35                    microalgae; however the industrial production of biodiesel is still far from becoming a  
36                    consolidated technology (Chisti, 2007; Brennan and Owende, 2010).

37                    Another biotechnological application of microalgae is their use for wastewater  
38                    treatment. Since the late 1950s, the growth of mixed consortia of microalgae and  
39                    bacteria has been promoted in high rate algal ponds (HRAP) with that aim. In these  
40                    treatment systems microalgae provide the required oxygen for the degradation of certain  
41                    wastewater constituents by aerobic bacteria. Though the interest in this  
42                    technology decreased over the years, in the current context of energy crisis it is

43 skyrocketing again due to its dual benefit: treating wastewater and producing algal  
44 biomass that can be valorised in the form of biofuels or bioproducts (Park et al., 2011).

45 All these microalgal biotechnology applications require tools that allow us  
46 to forecast biomass production in order to ensure feasibility for valorisation of  
47 microalgae as products or biofuels (Béchet et al., 2013). At the same time  
48 production forecasting is challenging because microalgae growth depends on many  
49 parameters such as solar radiation, nutrients availability (e.g. carbon and nitrogen) as  
50 well as on certain inhibitory conditions (e.g. excess of oxygen in the algal culture).

51 Mathematical models offer a great opportunity to study the simultaneous effect  
52 of different factors affecting algal growth and allow forecasting algal  
53 production. Research on microalgae growth kinetics modeling started with the  
54 pioneering work by Droop (1968, 1974). Since then a number of researchers have  
55 developed models based on single factors such as light intensity (Huisman, 1999),  
56 temperature (Franz et al., 2012), nitrogen (Bernard et al., 2009) and photosynthesis and  
57 photoinhibition effects (Wu and Merchuk, 2001). In fact, there is a vast array of models  
58 that predict biomass production as a function of light intensity (Yuan et al., 2014). This  
59 results from the fact that light cannot be easily controlled at full-scale microalgae  
60 cultures, in contrast to other factors which are maintained at optimal conditions to avoid  
61 limiting or inhibitory effects (e.g. pH, nutrients and mixing conditions).  
62 Recently, models of increasing complexity with two or more factors have been  
63 developed (Packer et al., 2011; Bonachela et al., 2011). As an example, in the model by  
64 Bernard (2011) light intensity and nitrogen are the limiting factors for microalgae  
65 growth. Most of these previous models use few parameters to describe the inherent  
66 complexity of algal cultures, especially so in the particular case of microalgae grown in  
67 wastewaters, where carbon and nitrogen limitations can be significant. Therefore the  
68 main objective of this paper is to present a new mechanistic model that includes  
69 crucial physical and biokinetic processes for the description of microalgae growth in  
70 different types of cultures, and most particularly in wastewater.

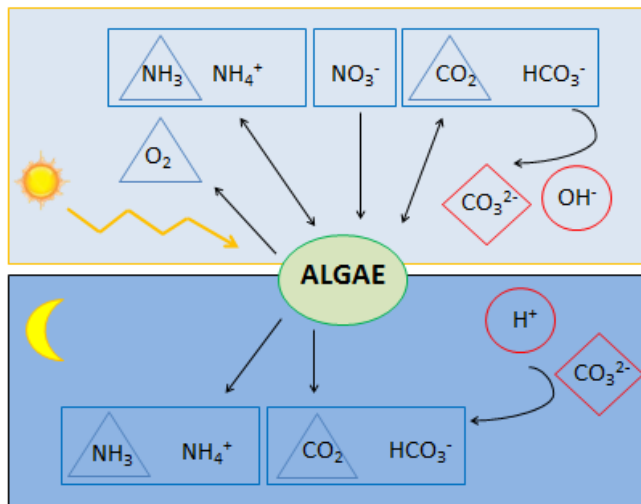
71 The main source of inspiration for building the presented model was the River  
72 Water Quality Model 1 (RWQM1) of the International Water Association (Reichert et  
73 al., 2011). RWQM1 was selected because it belongs to a family of widely accepted  
74 models (e.g. the Activated Sludge Models (ASM)) which share the same presentation,  
75 notation and structure for compounds, processes, and kinetic constants (Henze et al.,  
76 2000; Sah et al., 2011). Moreover, RWQM1 is the unique in the IWA family models  
77 because it considers microalgae activity.

78 The model was implemented in the COMSOL Multiphysics<sup>TM</sup> software, which  
79 solves differential equations using the finite elements method (FEM). For calibration we  
80 used experimental data obtained from a culture medium simulating treated urban  
81 wastewater (i.e. secondary effluent). This model will provide new insight into the  
82 functioning of microalgae cultures, and will help to explore the simultaneous effects of  
83 factors affecting microalgae growth. It is also a part of a more ambitious project  
84 through which we intend to develop a complete model to simulate mixed cultures of  
85 microalgae and bacteria treating wastewater (like HRAP or photobioreactors).

## 86 2. Model description

### 87 2.1 Conceptual model

88 The conceptual understanding that we have of the modelled system is shown in  
89 Figure 1. This figure shows that microalgae grow with light, consume substrates (i.e.  
90 carbon and nitrogen) and release oxygen. Note that other nutrients (e.g. phosphorus) and  
91 micronutrients are not considered to be limiting factors because are usually highly  
92 available in wastewater (which is the type of culture that mainly addresses the present  
93 model)(Larsdotter, 2006)As a result of microalgal activity,hydroxide ions concentration  
94 and pH increase. Increasing pHs displace the equilibrium of the carbon species towards  
95 the formation of carbonates. In darkness, endogenous respiration and inactivation of  
96 microalgae release carbon dioxide, the concentration of hydrogen ions increase and pH  
97 decreases. By decreasing pH the carbon equilibrium shifts and carbonate returns into  
98 bicarbonate, which can be used as substrate again in the presence of light.



99

100 Figure 1. General schematic representation of the conceptual model. Microalgae (green ellipse), substrates  
101 (rectangles), gaseous species (triangles) and species depending on algal activity which are neither substrates nor gases  
102 (diamonds and circles). Other nutrients (e.g. phosphorus) and micronutrients are not limiting factors.

### 103 2.2. Model components

104 The model follows the most commonly used nomenclature in the IWA models  
105 and considers 10 components. From these components, there are 9 dissolved  
106 components and one particulate component corresponding to microalgae biomass  
107 ( $X_{ALG}$ ).

#### 108 Dissolved components

- 109 1.  $S_{NH4}$  [ $gNH_4^+-N/m^3$ ]: Ammonium nitrogen. Nitrogen present in the water as ammonium.  
110 It is produced through the processes of endogenous respiration and through  
111 inactivation of microalgae. It is consumed through the growth of microalgae.

- 112 2.  $S_{NH_3}$  [gNH<sub>3</sub>-N/m<sup>3</sup>]: *Ammonia nitrogen*. Nitrogen in the form of ammonia. It is in  
 113 chemical equilibrium with ammonium ( $S_{NH_4}$ ). Its concentration decreases by  
 114 volatilization to the atmosphere.
- 115 3.  $S_{NO_3}$  [gNO<sub>3</sub><sup>-</sup>- N/m<sup>3</sup>]: *Nitrate nitrogen*. Nitrogen available as nitrate. It is consumed by  
 116 microalgae ( $X_{ALG}$ ).
- 117 4.  $S_{O_2}$  [gO<sub>2</sub>/m<sup>3</sup>]: *Dissolved oxygen*. Concentration of dissolved oxygen in the water. It is  
 118 produced by the growth of microalgae due to photosynthesis and consumed during  
 119 the processes of endogenous respiration and inactivation of microalgae. It can also be  
 120 transferred to the atmosphere.
- 121 5.  $S_{CO_2}$  [gCO<sub>2</sub>-C/m<sup>3</sup>]: *Carbondioxide*. Carbon as carbondioxide. It is consumed by  
 122 microalgae and is produced through the processes of endogenous respiration and  
 123 inactivation. Moreover, it is in chemical equilibrium with bicarbonate ( $S_{HCO_3}$ ) and  
 124 carbonate ( $S_{CO_3}$ ), and like dissolved oxygen ( $S_{O_2}$ ), it can be transferred to the  
 125 atmosphere.
- 126 6.  $S_{HCO_3}$  [gHCO<sub>3</sub><sup>-</sup>-C/m<sup>3</sup>]: *Bicarbonate*. Carbon as bicarbonate. It is in chemical  
 127 equilibrium with carbon dioxide ( $S_{CO_2}$ ) and carbonate ( $S_{CO_3}$ ). It is consumed by  
 128 microalgae.
- 129 7.  $S_{CO_3}$  [gCO<sub>3</sub><sup>2-</sup>-C/m<sup>3</sup>]: *Carbonate*. Carbon in the form of dissolved carbonate. It is in  
 130 chemical equilibrium with bicarbonate ( $S_{HCO_3}$ ) and carbon dioxide ( $S_{CO_2}$ ). Carbonate  
 131 is not used by microalgae as carbon source.
- 132 8.  $S_H$  [gH/m<sup>3</sup>]: *Hydrogen ions*. Concentration of hydrogen ions in the water. They are  
 133 involved in carbon and ammonium equilibrium systems. The concentration of  
 134 hydrogen ions decreases with the growth of microalgae and increases with  
 135 endogenous respiration and inactivation.
- 136 9.  $S_{OH}$  [gOH<sup>-</sup>-H/m<sup>3</sup>]: *Hydroxide ions*. Concentration of hydroxide ions in the water.  
 137 They are in equilibrium with hydrogen ions.

### 138 **Particulate components**

- 139 10.  $X_{ALG}$  [gCOD/m<sup>3</sup>]: *Microalgae biomass*. Concentration of microalgae. It increases  
 140 with growth processes and decreases by endogenous respiration and inactivation.  
 141 Note that it is expressed in gCOD (chemical oxygen demand)/m<sup>3</sup> as it is common  
 142 practice to express organic matter concentrations in all IWA models. Microalgae  
 143 biomass is transformed from COD to TSS (total suspended solids) assuming a ratio  
 144 COD/TSS= 0.80 (Sperling, 2007; Khorsandi et al., 2014).

### 145 **2.3.Processes**

146 Table 1 shows a list of the processes included in the model and the equations  
 147 describing their rates. Table 2 shows the matrix of stoichiometric parameters.

148

149

150

151

152

153

154

155

156

157

158

159

160

161  
162

Table 1. Mathematical description of the processes of the model (processes rates).

Processes	Process rate [M L <sup>-3</sup> T <sup>-1</sup> ]
1a. Microalgae growth on ammonia	$\rho_{1a} = \mu_{ALG} * f_{T,FS}(T) * \eta_{PS}(I, S_{O2}) * \frac{S_{CO2} + S_{HCO3}}{K_{C,ALG} + S_{CO2} + S_{HCO3} + \frac{S_{CO2}^2}{I_{CO2,ALG}}} * \frac{S_{NH3} + S_{NH4}}{K_{N,ALG} + S_{NH3} + S_{NH4}} * X_{ALG}$
1b. Microalgae growth on nitrate	$\rho_{1b} = \mu_{ALG} * f_{T,FS}(T) * \eta_{PS}(I, S_{O2}) * \frac{S_{CO2} + S_{HCO3}}{K_{C,ALG} + S_{CO2} + S_{HCO3} + \frac{S_{CO2}^2}{I_{CO2,ALG}}} * \frac{S_{NO3}}{K_{N,ALG} + S_{NO3}} * \frac{K_{N,ALG}}{K_{N,ALG} + S_{NH3} + S_{NH4}} * X_{ALG}$
2. Microalgae endogenous respiration	$\rho_2 = k_{resp,ALG} * f_{T,FS}(T) * \frac{S_{O2}}{K_{O2,ALG} + S_{O2}} * X_{ALG}$
3. Microalgae inactivation	$\rho_3 = k_{deat,h,ALG} * f_{T,FS}(T) * X_{ALG}$
4. Chemical equilibrium $CO_2 \leftrightarrow HCO_3^-$	$\rho_4 = k_{eq,1} * (S_{CO2} - \frac{S_H S_{HCO3}}{K_{eq,1}})$
5. Chemical equilibrium $HCO_3^- \leftrightarrow CO_3^{2-}$	$\rho_5 = k_{eq,2} * (S_{HCO3} - \frac{S_H S_{CO3}}{K_{eq,2}})$
6. Chemical equilibrium $NH_4^+ \leftrightarrow NH_3$	$\rho_6 = k_{eq,3} * (S_{NH4} - \frac{S_H S_{NH3}}{K_{eq,3}})$
7. Chemical equilibrium $H^+ \leftrightarrow OH^-$	$\rho_7 = k_{eq,w} * (1 - \frac{S_H S_{OH}}{K_{eq,w}})$
8. Oxygen transfer to the atmosphere	$\rho_{O2} = Ka_{,O2} * (S_{O2}^{WAT} - S_{O2})$
9. Carbon dioxide transfer to the atmosphere	$\rho_{CO2} = Ka_{,CO2} * (S_{CO2}^{WAT} - S_{CO2})$
10. Ammonia transfer to the atmosphere	$\rho_{NH3} = Ka_{,NH3} * (S_{NH3}^{WAT} - S_{NH3})$

163  
164  
165  
166  
167  
168

169  
170

Table 2. Matrix of stoichiometric parameters that relates processes and components through stoichiometric coefficients in Supplementary Table 3.

State variables $\rightarrow i$		$S_{NH4}$	$S_{NH3}$	$S_{NO3}$	$S_{O2}$	$S_{CO2}$	$S_{HCO3}$	$S_{CO3}$	$S_H$	$S_{OH}$	$X_{ALG}$
Processes $\downarrow j$		$gN/m^3$	$gN/m^3$	$gN/m^3$	$gO_2/m^3$	$gC/m^3$	$gC/m^3$	$gC/m^3$	$gH/m^3$	$gH/m^3$	$gCOD/m^3$
1a. Microalgae growth on ammonia	$\rho_{1a}$	$v_{1,1a}$			$v_{4,1a}$	$v_{5,1a}$			$v_{8,1a}$		$v_{10,1a}$
1b. Microalgae growth on nitrate	$\rho_{1b}$			$v_{3,1b}$	$v_{4,1b}$	$v_{5,1b}$			$v_{8,1b}$		$v_{10,1b}$
2. Microalgae endogenous respiration	$\rho_2$	$v_{1,2}$			$v_{4,2}$	$v_{5,2}$			$v_{8,2}$		$v_{10,2}$
3. Microalgae inactivation	$\rho_3$	$v_{1,3}$			$v_{4,3}$	$v_{5,3}$			$v_{8,3}$		$v_{10,3}$
4. Chemical equilibrium $CO_2 \leftrightarrow HCO_3^-$	$\rho_4$					$v_{5,4}$	$v_{6,4}$		$v_{8,4}$		
5. Chemical equilibrium $HCO_3^- \leftrightarrow CO_3^{2-}$	$\rho_5$						$v_{6,5}$	$v_{7,5}$	$v_{8,5}$		
6. Chemical equilibrium $NH_4^+ \leftrightarrow NH_3$	$\rho_6$	$v_{1,6}$	$v_{2,6}$						$v_{8,6}$		
7. Chemical equilibrium $H^+ \leftrightarrow OH^-$	$\rho_7$								$v_{8,7}$	$v_{9,7}$	
8. Oxygen transfer to the atmosphere	$\rho_{O2}$				$v_{4,02}$						
9. Carbon dioxide transfer to the atmosphere	$\rho_{CO2}$					$v_{5,CO2}$					
10. Ammonia transfer to the atmosphere	$\rho_{NH3}$		$v_{2,NH3}$								

171

172 **Algal processes**

173 - *Growth of microalgae*(processes 1a and 1b in Table 1).The increase of microalgae  
 174 biomass per unit of time (growth rate) is expressed as the product of their maximum  
 175 specific growth rate ( $\mu_{ALG}$ ) by their concentration at that point in time( $X_{ALG}$ ) and by  
 176 correctiv factors (in the form of Monod functions) that limit or inhibit their growth.

177 Microalgae grow with both carbon dioxide ( $S_{CO2}$ ) and bicarbonate ( $S_{HCO3}$ ). Note  
 178 that in the matrix of stoichiometric parameters (Table 2) only the reaction rate of  
 179 carbondioxide is affected by microalgae growth because the concentration of  
 180 bicarbonate is already in chemical equilibrium with it. Carbon dioxide ( $S_{CO2}$ ) inhibits  
 181 microalgae growth at very high concentrations based on the results of Silva and  
 182 Pirt(1984). More precisely, it has been observed that in closed photobioreactors  $CO_2$   
 183 behaves as an inhibitor at partial pressures above 0.6 atm, which is equivalent to a  
 184 dissolved  $CO_2$  concentration of 440 mg $CO_2$ /L at 37 °C (Silva and Pirt, 1984). Inhibition  
 185 caused by  $CO_2$  is due to the compound itself as well as its effect on acidity, which in the  
 186 current status of the model can not be distinguished. Microalgae grow with ammonia and  
 187 ammonium ( $S_{NH4} - S_{NH3}$ ) or with nitrate ( $S_{NO3}$ ) as nitrogen source. When ammonium (or  
 188 ammonia, note that they are in chemical equilibrium) and nitrate are both present,  
 189 ammonium is generally preferred (Stewart, 1974; Syrett, 1981; Monstert and Grobbelar,  
 190 1987). To represent this phenomenon, the highlighted term that describes the inhibiting  
 191 effect of ammonia and ammonium on growth of microalgae once nitrate has been  
 192 introduced in Eq. (1) (process 1b in Table 1).

193

194 
$$\rho_{1b} = \mu_{ALG} * f_{T,FS}(T) * \eta_{PS}(I, S_{O2}) * \frac{S_{CO2} + S_{HCO3}}{K_{C,ALG} + S_{CO2} + S_{HCO3} + \frac{S_{CO2}^2}{I_{CO2,ALG}}} * \frac{S_{NO3}}{K_{N,ALG} + S_{NO3}} * \frac{K_{N,ALG}}{K_{N,ALG} + S_{NH3} + S_{NH4}} * X_{ALG} (1)$$

195

196 Here again note that microalgae growth only affects the reaction rate of ammonia  
 197 because it is in equilibrium with ammonium (Table 2).

198 The photosynthetic factor ( $\eta_{PS}$ ) takes into account the effects of light intensity ( $I$ )  
 199 and excess of oxygen ( $S_{O2}$ ) on photosynthesis and therefore on microalgae growth. The  
 200 following relationship was introduced:

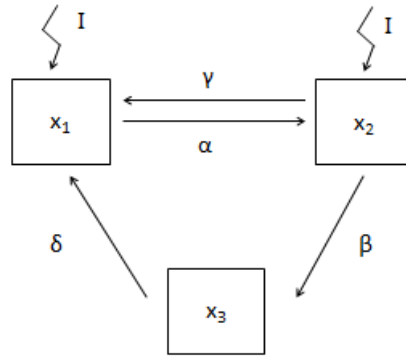
201

$$\eta_{PS}(I, S_{O2}) = f_L(I) \cdot f_{PR}(S_{O2}) \quad (2)$$

202 where,  $f_L$  is the light factor and  $f_{PR}$  the photorespiration factor.

203 The effects of light intensity on photosynthesis are described by the  
 204 ‘photosynthetic factories’ model (PSF) as proposed by Eilers and Peeters (1988): at low  
 205 light irradiance, the rate of photosynthesis is proportional to light intensity because  
 206 photosynthesis is limited by the rate of capture of photons. When irradiance increases to  
 207 a certain point, microalgae become ‘light saturated’ because photosynthesis cannot  
 208 process more photons. If irradiance increases beyond an inhibitory threshold, the rate of  
 209 photosynthesis starts to decrease (Crill, 1977; Camacho-Rubio et al., 2003; Béchet et  
 210 al., 2013).

211 In the PSF model it is assumed that microalgae are present in three different  
 212 states: resting or ‘open’ ( $x_1$ ), activated or ‘closed’( $x_2$ ), and inhibited ( $x_3$ ) (Figure 2).  
 213



214

215 Figure 2. Three different states and relationships of the photosynthetic factories model (PSF): open ( $x_1$ ),  
 216 closed ( $x_2$ ) and inhibited ( $x_3$ ) (Adapted from Eilers and Peeters(1998)).

217

218 Initially microalgae are in open state  $x_1$ , ready to capture a photon. When the  
 219 photon is captured and biochemical reactions start, microalgae turn to activated state  $x_2$ .  
 220 This reaction depends on the rate of activation  $\alpha$   
 221  $[(\mu\text{E}/\text{m}^2)^{-1}]$ . In activated state microalgae can go back to open state  $x_1$  in dark conditions,  
 222 or can capture another photon and pass to inhibited state  $x_3$ . These two reactions depend  
 223 on a rate constant of production  $\gamma[\text{s}^{-1}]$  and on a rate constant of inhibition  $\beta[(\mu\text{E}/\text{m}^2)^{-1}]$ .  
 224 Microalgae in the inhibited state turn back to the open state with a rate of recovery  
 225  $\delta[\text{s}^{-1}]$ .

226 Considering the principle of mass conservation, the three states can be described  
 227 by the following system of differential equations (Equation 3, 4, 5 and 6):

228

229 
$$\frac{dx_1}{dt} = -\alpha \cdot I \cdot x_1 + \gamma \cdot x_2 + \delta \cdot x_3 \quad (3)$$

230 
$$\frac{dx_2}{dt} = \alpha \cdot I \cdot x_1 - \gamma \cdot x_2 - \beta \cdot I \cdot x_2 \quad (4)$$

231 
$$\frac{dx_3}{dt} = \beta \cdot I \cdot x_2 - \delta \cdot x_3 \quad (5)$$

232 
$$x_1 + x_2 + x_3 = 1 \quad (6)$$

233

234 When irradiance is not constant, but is a nonlinear function of time ( $I(t)$ ), this  
 235 system of differential equations does not have an analytical solution. However, under  
 236 outdoor conditions, variations of  $I$  during the daily solar cycle are very slow with respect  
 237 to the dynamics of photosynthesis (Eilers and Peeters, 1988, Camacho-Rubio et al.,  
 238 2002,). In these conditions  $x_1$  and  $x_2$  are close to equilibrium within less than a second.  
 239 Therefore it can be assumed that equilibrium is reached instantly, making the left hand  
 240 side of differential terms equal to zero. Under this assumption, the solution to this  
 241 system of differential equations is:

242

243 
$$x_1 = \frac{\gamma\delta + \beta I\delta}{\alpha\beta I^2 + (\alpha + \beta)\delta I + \gamma\delta} \quad (7)$$

244 
$$x_2 = \frac{\alpha\delta I}{\alpha\beta I^2 + (\alpha + \beta)\delta I + \gamma\delta} \quad (8)$$

245  $x_3 = \frac{\alpha\beta I^2}{\alpha\beta I^2 + (\alpha + \beta)\delta I + \gamma\delta}$  (9)

246

247 The state in which microalgae can grow is  $x_2$ , and therefore in our model the  
248 photosynthetic factor is:

$$f_L(I) = x_2 \quad (10)$$

249

250 As shown before (Eq. 2), in microalgae cultures photosynthesis not only depends  
251 on the solar irradiance, but is also a function of oxygen concentration (for high  
252 concentrations). Especially in closed photobioreactors where there is little (if any)  
253 oxygen exchange with the atmosphere, the accumulation of this component may inhibit  
254 photosynthesis (Molina-Grima et al., 2001). According to Chisti (2007), to prevent  
255 such inhibitory effects the dissolved oxygen concentrations should never exceed about  
256 400% of air saturation value. The photorespiration factor is introduced in this work  
257 to represent this phenomenon in mathematical terms:

258

259 
$$f_{PR}(S_{O_2}) = \begin{cases} 1 - \tanh\left(\frac{K_{PR} \frac{S_{O_2}}{\tau \cdot S_{O_2}^{SAT}}}{1 - \frac{S_{O_2}}{\tau \cdot S_{O_2}^{SAT}}}\right), & S_{O_2} \leq \tau \cdot S_{O_2}^{SAT} \\ 0, & S_{O_2} > \tau \cdot S_{O_2}^{SAT} \end{cases} \quad (11)$$

260

261 where  $S_{O_2}^{SAT}$  [gO<sub>2</sub>/m<sup>3</sup>] is the saturation concentration of oxygen in the air. The  
262 photorespiration inhibition constant ( $K_{PR}$ ) and the coefficient of excess dissolved  
263 oxygen ( $\tau$ ) are parameters that have to be calibrated during the application of the model.

264 The effect of photorespiration does not affect microalgal production if the  
265 concentration of oxygen in water is clearly lower than  $\tau$  times the saturation  
266 concentration, as is the case of open photobioreactors (Chisti, 2007). However, when the  
267 concentration of oxygen tends towards saturation ( $\tau S_{O_2}^{SAT}$ ) the photorespiration factor  
268 decreases, hindering microalgae growth.

269 The thermic photosynthetic factor ( $f_{T,FS}$ ) takes into account the effects of  
270 temperature on microalgae growth and also on endogenous respiration and inactivation  
271 processes (1a, 1b, 2 and 3 in Table 1, respectively). Water temperature varies on both  
272 diurnal and seasonal scales, affecting both microalgal photosynthesis and respiration  
273 rates. The optimal temperature for algal growth ranges between 15°C and 25°C,  
274 depending on the species (Larsdotter, 2006; Bitog et al., 2011). The thermic  
275 photosynthetic factor is represented in the model following the work of Dauta et al.  
276 (1990):

277

278 
$$f_{T,FS}(T) = e^{-\left(\frac{T - T_{opt}}{s}\right)^2} \quad (12)$$

279 where  $T_{opt}$  was assumed equal to 25 °C (Dauta et al., 1990) and  $s$  is a parameter  
280 value for empirical fitting.

281 -*Endogenous respiration*(process 2 in Table 1). The rate of this process is expressed as  
 282 the product between the maximum rate of endogenous respiration ( $k_{resp,alg}$ ), the  
 283 concentration of microalgae, the thermic photosynthetic factor(the same as used for the  
 284 growth of microalgae) and Monod function relates limiting oxygen concentration to a  
 285 microalgae growth rate.

286 - *Inactivation of microalgae*(process 3 in Table 1). The rate of this process is expressed  
 287 as the product of the maximum rate of inactivation ( $k_{death,alg}$ )by the concentration of  
 288 microalgae and by thermic photosynthetic factor (the same as for growth) (Reichert et  
 289 al., 2001).

## 290 **Chemical equilibrium reactions**

291 Chemical equilibria affect carbon, nitrogen and the balance of hydrogen and  
 292 hydroxide ions (processes 4, 5, 6 and 7 in Table 1). The rates of these chemical  
 293 reactions ( $\rho_i$ ) [ $\text{g}\cdot\text{m}^{-3}\cdot\text{d}^{-1}$ ] are obtained with the following general equation(Batstone et  
 294 al., 2002):

$$295 \rho_i = K_{eq,i}(S_i - S_{eq,i}) \quad (13)$$

297 Where  $i=1 \dots n$  and  $n$  is the number of chemical species in equilibrium,  $K_{eq,i}$  [ $\text{d}^{-1}$ ] is  
 298 the dissociation constant of reaction  $i$ ,  $S_i$  [ $\text{g}/\text{m}^3$ ] is the concentration of the  $i^{\text{th}}$  component  
 299 and  $S_{eq,i}$  [ $\text{g}/\text{m}^3$ ] is the concentration at equilibrium.

## 300 **Transfer of gases to the atmosphere**

302 Transfer rates of oxygen, carbon dioxide and ammonia between water and the  
 303 atmosphere (processes 8, 9 and 10 in Table 1) are given by the general  
 304 equation(Batstone et al., 2002):

$$305 \rho_j = K_{a,j}(S_j^{WAT} - S_j) \quad (14)$$

307 where  $j=1 \dots m$  and  $m$  is the number of transfer rates,  $S_j^{WAT}$  [ $\text{g}/\text{m}^3$ ] is the saturation  
 308 concentration of  $j^{\text{th}}$  gas in the water,  $S_j$  [ $\text{g}/\text{m}^3$ ] is the gas concentration in the water and  $K_{a,j}$   
 309 is the overall mass transfer coefficient of  $j^{\text{th}}$  gas [ $\text{d}^{-1}$ ].  $K_a$  depends on the temperature, the  
 310 nature of the gas and the liquid and the extension of the surface interface.

## 312 **2.4. Effects of temperature, irradiance and pH**

314 Temperature, irradiance and pH also affect the rates the processes described  
 315 previously.

316 **Irradiance ( $I(\lambda)$ )** [ $\mu\text{E}/(\text{m}^2\cdot\text{s})$ ]: Wavelength-specific *Irradiance or light intensity*. It is also  
 317 known in literature as a photon flux density (PFD).

318 In the present model irradiance was expressed as photosynthetically active  
 319 radiation (PAR), which includes wavelengths between 400 and 700 nm (Zonneveld,  
 320 1998):

321

$$322 \quad \text{PAR} = \int_{400 \text{ nm}}^{700 \text{ nm}} I(\lambda) d\lambda \quad (15)$$

323

324 If measured PAR values are not available, estimated values at any Earth  
 325 geographical location can be calculated from coordinates with the equations presented  
 326 in Table 3 (Al-Rawahi et al., 2011).

327

328 Table 3 - Mathematical equations for estimating irradiance at any point on Earth. Parameters and factors are  
 329 described in Supplementary Table 1.

330

Description	Mathematical Equation	Units
Total incident solar irradiation	$I_0 = \frac{\pi H E_f}{24} \{ [0.409 + 0.5016 \cdot \sin(\omega_s - 60)]$ $+ [0.6609 - 0.4767 \cdot (\omega_s - 60)] \cos \omega \}$ $\times \left( \frac{\cos \omega \cdot \cos \omega_s}{\sin \omega_s - \omega_s \cdot \cos \omega_s} \right) \cdot 0,2174$	$\mu\text{E}/(\text{m}^2\text{s})$
Daily radiation	$H = \kappa H_0$	$\text{J}/(\text{m}^2\text{d})$
Total daily extraterrestrial radiation	$H_0 = \left( \frac{24\zeta}{\pi} \right) \left( 1 + 0.003 \cdot \cos \left( \frac{360 N}{365} \right) \right) \left( \cos \phi \cdot \cos \delta \cdot \sin \omega_s + \frac{2\pi\omega_s}{360} \right.$ $\left. \cdot \sin \phi \cdot \sin \delta \right)$	$\text{J}/(\text{m}^2\text{d})$

331

332 **Water temperature (T[°C]):** *Watertemperature*. Microalgae processes are influenced  
 333 by temperature described by thermic photosynthetic factor Eq. (12).

334

335 **pH[-].** pH of the aqueous medium is obtained from hydrogen ions concentration  
 336 ( $S_H$ ). pH value displaces the equilibrium of the carbon and nitrogen species.

### 337 2.5. Stoichiometry and parameter values

338 The stoichiometric matrix is presented in Table 2 and is based on the structure of  
 339 IWA models (Petersen matrix). Values of biokinetic, physical and chemical parameters  
 340 are shown in Supplementary Tables 1-2. Mathematical expressions of the stoichiometric  
 341 coefficients of each process are shown in Supplementary Table 3-4.

342

343 Using Tables 1 and 2, the reaction rate for each component of the model ( $r_i$ ) is obtained  
 344 with:

345

$$r_i = \sum_j v_{j,i} * \rho_j \quad (15)$$

346

347 where  $i$  is the number of components and  $j$  is the number of processes;  $\rho_j$  is the  
 348 reaction rate for each process  $j$  and  $v_{j,i}$  is the stoichiometric coefficient. The expressions  
 349 of stoichiometric coefficients related to microalgae processes are based on the fractions  
 350 of carbon ( $i_{C,ALG}$ ), hydrogen ( $i_{H,ALG}$ ), oxygen ( $i_{O,ALG}$ ) and nitrogen ( $i_{N,ALG}$ ) (Appendix,  
 Table 6 and 7).

### 351 3. Experimental verification

352 Experiments were carried out in a batch mesocosm microalgae culture located  
353 outdoors at the facilities of the Laboratory of Environmental Biotechnology (LBE,  
354 INRA) in Narbonne, South of France (43°11'N, 3°00'E, 13 m A.M.S.L.).The mesocosm  
355 consisted of a cylindrical PVC container with a surface area of 1.30 m<sup>2</sup> and a depth of  
356 0.55 m (nominal volume 500 L).A drainage pump ensured continuous stirring of culture  
357 medium.

358 Experiments started on January 23<sup>rd</sup> 2012. The mesocosm (without replicates)  
359 was manually filled with 450 L of medium. 50 L of inoculum with the microalgae  
360 *Scenedemussp* were added. The medium was prepared as to simulate the mineral  
361 composition of a wastewater. A commercial mineral fertilizer (Antys8, Frayssinet,  
362 France)(80 g/LTN, 50 g/LP<sub>2</sub>O<sub>5</sub>) was diluted into tap water (0.16/1000), and 0.03g/L of  
363 NH<sub>4</sub>Cl were added to increase nitrogen concentration. The experiments lasted 9 days,  
364 and no new fresh medium was added during the entire experimental period.

365  
366 Photosynthetically active radiation (PAR) was measured with a probe (Sky  
367 Instruments PAR Quantum Sensor) located on the surface of mesocosms; data were  
368 recorded every five minutes. Water temperature and pH were measured with pH and  
369 temperature probes (InPro 426i, Mettler Toledo, CH) every morning. During the 9 days  
370 water temperature varied between 9 and 18.7 °C (January and February are the coldest  
371 months in the region) and the light intensity (PAR) ranged from 3.25 and 655 μE/m<sup>2</sup>\*s.

372 Samples of the microalgae culture were taken after 2, 4, 8 and 9 days, and  
373 analyzed for total suspended solids (TSS) as indicator of algal biomass and ammonium  
374 (NH<sub>4</sub><sup>+</sup>-N) according to conventional procedures indicated in the Standard Methods  
375 (APHA-AWWA-WPCF, 2001).

### 376 4. Model implementation and calibration procedure

377 The model described in section 2 was implemented in COMSOL  
378 Multiphysics<sup>TM</sup> v4.3b software. A 0D domain was used to represent the experimental  
379 reactor (mesocosms), which can be considered in perfect mixing, and therefore transport  
380 of aqueous phase species (i.e. dissolved and particulate) can be ignored.

381 The model was calibrated using available data for the 9 days of experimentation.  
382 Manual trial and error adjustment of parameters was used to match measured data as  
383 much as possible using graphical representations.

384 The concentrations of components in the mesocosms measured at the beginning  
385 of the experiment are shown in Table 3.

386

Table 3. Initial concentrations of the components in the mesocosms.

Component	Concentration	Units
<b>Dissolved Components</b>		
S <sub>NH4</sub>	8.1	gN-NH <sub>4</sub> /m <sup>3</sup>
S <sub>NH3</sub>	0.685	gN-NH <sub>3</sub> /m <sup>3</sup>

$S_{NO3}$	11.37	$gN-NO_3/m^3$
$S_{CO2}$	0.8	$gC-CO_2/m^3$
$S_{HCO3}$	100	$gC-HCO_3/m^3$
$S_{CO3}$	1.17	$gC-CO_3/m^3$
$S_{O2}$	8	$gO_2/m^3$
$S_H$	$3.16*10^{-6}$	$gH/m^3$
$S_{OH}$	$2.83*10^{-3}$	$gH-OH/m^3$
<b>Particulate Component</b>		
$X_{ALG}$	100	$gTSS/m^3$

387

388

389

390

391

392

393

394

395

396

397

From the 31 parameters implemented in the model, 16 parameters were obtained from the existing River Water Quality Model (Reichert et al., 2001). Those parameters related to transfer of gases to the atmosphere, temperature, photorespiration and carbon limitation on microalgae growth are not included into the RWQM1 and they were obtained from other literature cited in Tables. Morris's uncertainty method (Morris, 1991) was applied to screening which parameters had a greater influence on the simulation response. Based on a previous uncertainty analysis, the model was calibrated by adjusting the values of the maximum growth rate of microalgae ( $\mu_{ALG}$ ), the transfer of gases to the atmosphere and the photorespiration inhibition constant ( $K_{PR}$ ). Calibration was conducted by comparing simulated and experimental data curves.

398

## 5. Results

399

400

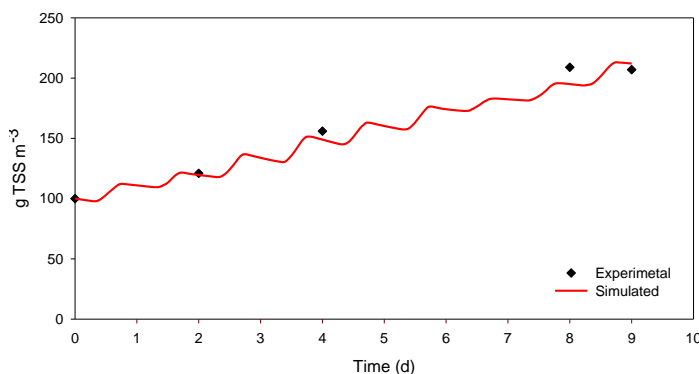
401

402

403

404

Biomass concentration in the mesocosm increased from 100  $gTSS/m^3$  at the beginning of the experiment to around 210  $gTSS/m^3$  after 9 days. Figure 3 shows that the model was able to reproduce such growth pattern with an acceptable accuracy. Interestingly, the simulated curve has a wavelike trend which indicates that the model is able to reproduce microalgae growth (crests) and inactivation (trough) cycles occurring during daytime and at night, respectively.



405

406

407

408

Figure 3. Experimental (black dots) and simulated (red line) microalgae biomass growth over the 9 days. The crests and troughs of the simulated curve correspond to microalgae growth and inactivation periods during daytime and at night, respectively.

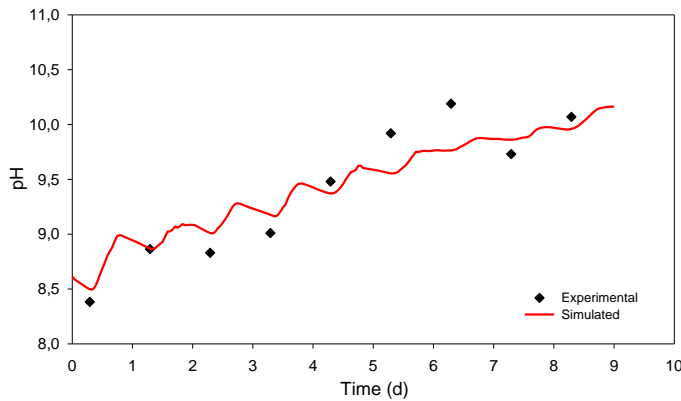
409

410

411

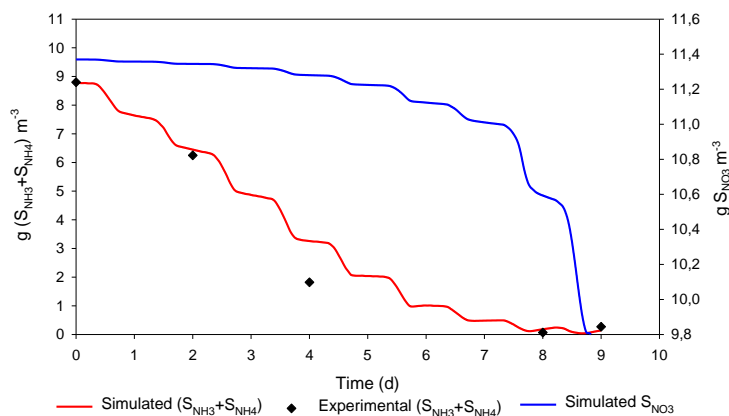
On the other hand, Figure 4 shows that pH increased with the growth of microalgae. Despite the fitting between experimental data and simulation results are not as good as in Figure 3, the model still predicts the general trend shown by the

412 experimentally measured pH values. Again, daily pH variations related to the activity of  
 413 microalgae can be clearly observed. In darkness, the pH decreases as a consequence of  
 414 endogenous respiration and inactivation of microalgae which release both carbon  
 415 dioxide and hydrogen ions, while during the day the pH increases due to photosynthesis.  
 416



417  
 418  
 419 Figure 4. Experimental (black dots) and simulated (red line) pH values over the 9 days period.  
 420

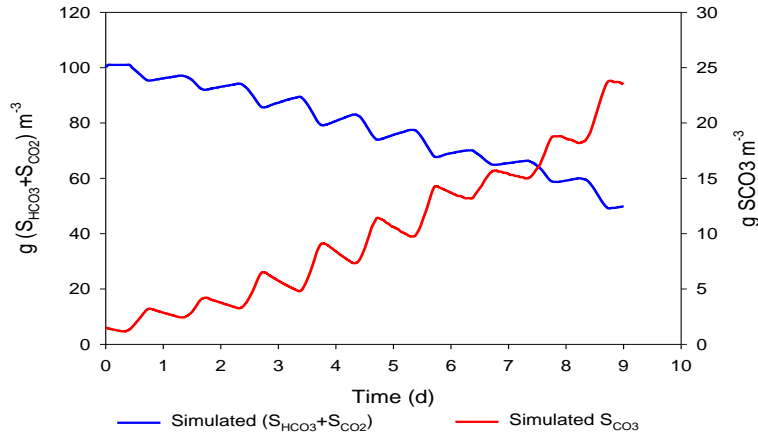
421 Figure 5 shows the experimental and simulated ammonium nitrogen  
 422 concentrations within the mesocosm as well as the simulated nitrate concentration (note  
 423 that nitrate concentrations were not measured in the experimental study). Once more,  
 424 the simulated ammonium concentrations match the trend of the experimental  
 425 measurements with a satisfactory degree of accuracy. Although this phenomenon cannot  
 426 be demonstrated with the available experimental data, Figure 5 also shows to what  
 427 extent microalgae growth used ammonium preferably to nitrate as nitrogen source. After  
 428 6 days, the concentrations of  $S_{NH_4}$  and  $S_{NH_3}$  were very low but microalgae continued  
 429 growing, most likely by consuming  $S_{NO_3}$ . Once again, the daily  $S_{NH_4}+S_{NH_3}$  variations  
 430 related to the activity of microalgae can be clearly observed.



431  
 432 Figure 5. Comparison between experimental (dots) and simulated (red line) concentrations of ammonium and  
 433 ammonia and simulated concentrations of nitrate (blue line).  
 434

435 Figure 6 shows simulation results for  $S_{CO_2}+S_{HCO_3}$  and  $S_{CO_3}$  concentrations.  
 436  $S_{CO_2}+S_{HCO_3}$  decreased with the growth of microalgae while the concentration of

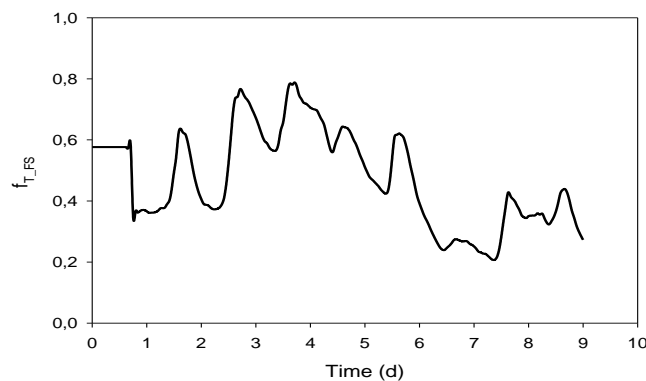
437  $S_{CO_3}$  followed the opposite trend. For increasing values of pH, the equilibrium of the  
 438 carbon species is displaced towards the formation of carbonates  $CO_3^{2-}$ . Daily variations  
 439 of these carbon species are again related to growth and endogenous respiration and  
 440 inactivation cycles during daytime and at night, respectively.



441  
 442  
 443  
 444

Figure 6. Microalgae uptake of carbon ( $S_{HCO_3} + S_{CO_2}$ ) (red line) and  $S_{CO_3}$  (blue line) simulated curves.

445 The thermic photosynthetic factor ( $f_{T,FS}(T)$ ) which depends exclusively on  
 446 temperature can range between 0 and 1, where higher values are favourable for algae  
 447 growth. According to Figure 7 at the beginning of the experimental study (first 5 days)  
 448 the conditions were more favourable for microalgae growth, and slightly worsened after  
 449 that (Figure 7). Temperature values (shown in Figure 8, from 9°C up to 18°C), give  
 450 values of the photosynthetic thermal factor oscillating between 0.38 and 0.8. Meanwhile  
 451 low temperature from day 6 to 9 (from 9°C up to 12°C) decreased microalgae activity.  
 452 This phenomenon can be observed by looking at the biomass growth rate (slope of the  
 453 curve of Figure 3), which decreases slightly after day 5.



454  
 455  
 456  
 457

Figure 7. Evolution of the thermic photosynthetic factor ( $f_{T,FS}$ ) over the 9 days of the experiment.

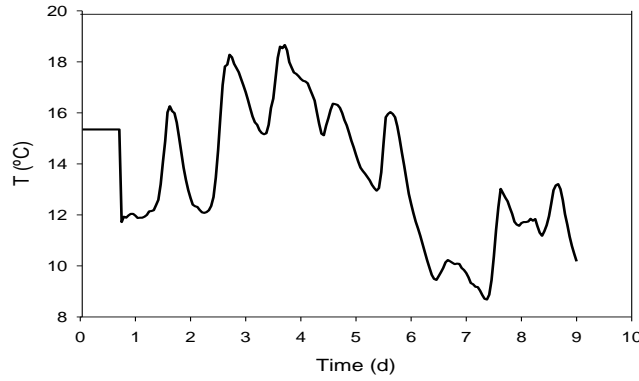


Figure 8. Temperature measurements ( $T$ ) over the 9 days of the experiment.

Table 4 presents the values of the parameters that were calibrated to obtain the results of Figures 3 to 7.

Table 4. Values of calibrated parameters.

Parameter	Description	Value
$\mu_{ALG}$	Maximum specific growth rate of microalgae	$1.5 \text{ d}^{-1}$
$K_{a,O_2}$	Mass transfer coefficient for oxygen	$4 \text{ d}^{-1}$
$K_{a,CO_2}$	Mass transfer coefficient for carbon dioxide	$0.6 \text{ d}^{-1}$
$K_{a,NH_3}$	Mass transfer coefficient for ammonia	$0.6 \text{ d}^{-1}$

## 6. Discussion

### 6.1 Innovative features of the model

The main innovation of the current model comes from considering inorganic carbon as a limiting substrate for the growth of microalgae. Previous research on microalgae growth modeling focused on properly describing the dependence of microalgae growth on light, while carbon limitation was not addressed (Wu and Merchuk, 2001; Franz et al., 2012). This approach was justified by the fact the growth of microalgae was studied in photobioreactors in which carbon dioxide was supplied through injection and thus carbon availability was always ensured (Bitog et al., 2011). However, microalgae grown in wastewater systems such as HRAP, in which no external carbon dioxide is supplied, are usually carbon limited (Buhr and Miller, 1983). Hence, in this case, it is essential to consider carbon limitation for a correct estimation of biomass production. In the scenario simulated in this work it was shown how the model was able to simulate the dynamics of the carbon species and in this case it was observed that they did not hinder algae growth. Carbon limitation was implemented in the model by introducing the correction factor  $K_{C,ALG}$  in the equation describing the growth rate of microalgae (processes 1a and 1b in Table 1).

486 On the other hand, excessively high concentrations of carbon dioxide can also be  
487 counter-productive and inhibit the growth of microalgae (Kurano and Miyachi,  
488 2005). Although in our experimental setup the excess of carbon dioxide is released to the  
489 atmosphere and does not inhibit algae growth, this effect has to be taken into account in  
490 closed reactors. To this end, the presented model also implements the inhibitory effect  
491 of high concentration of carbon dioxide through the parameter  $I_{CO_2,ALG}$  (Silva and Pirt,  
492 1984) (processes 1a and 1b in Table 1).

493 Temperature has also an effect on the chemical equilibrium of species, pH and  
494 gas solubility (Bouterfas et al., 2002). In the current scenario, when temperatures  
495 decreased, photosynthetic activity also decreased. It is translated into lower pH  
496 oscillations ( $\pm 0.2$ ) during the day/night cycle (Figure 4).

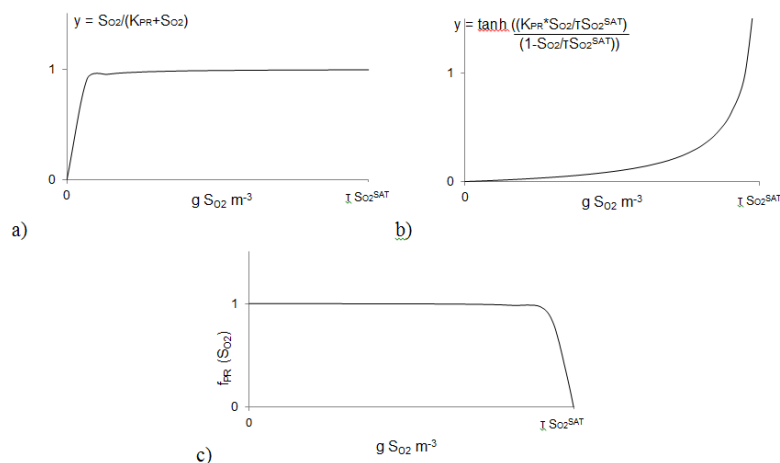
497 Photosynthetic processes (e.g. photoinhibition and  
498 photolimitation) and photorespiration phenomena were lumped together into a single  
499 parameter called the photosynthetic factor  $\eta_{PS}(I, S_{O_2})$ . Among others, the photosynthetic  
500 factor includes the influence of irradiance on microalgal growth. In fact, this parameter  
501 is considered the main limiting factor in microalgae systems (Larsdotter, 2006; Park and  
502 Craggs, 2011).

503 The dynamic model of photosynthesis and photoinhibition presented by Eilers  
504 and Peeters (1992) solves the system of differential equations 3 to 6 considering constant  
505 light intensity ( $I$ ). In the current work this approach was also adopted. To reproduce the  
506 daily variation of light intensity we assume that photosynthetic processes are fast  
507 compared to the rate of change of irradiance; hence, the activated photosynthetic factor  
508 ( $x_2$ ) quickly reaches equilibrium with instantaneous irradiance (Camacho-Rubio et al.,  
509 2002). This simplification was required to obtain the analytical solution of the system of  
510 differential equations (3-6).

511 The second term of the Equation (2)  $f_{PR}(S_{O_2})$  considers the effects of  
512 photorespiration on microalgae growth, a phenomenon so far never modelled in large-  
513 scale algal cultures. Chisti (2007) imposed a maximum concentration of oxygen  
514 dissolved in water equal to four times the value of air saturation. This concentration can  
515 be considered equal to  $7.1904 \text{ gO}_2/\text{m}^3$  (Rubio and Fernández, 1999). To this restriction  
516 must be added the fact that photorespiration phenomenon starts suddenly at high  
517 concentration of dissolved oxygen, without significant impact to low concentrations.

518 Despite the scarce information available on modelling photorespiration, a  
519 photorespiration factor  $f_{PR}(S_{O_2})$  has been proposed in the current work (Equation 11),  
520 representing the effects of high oxygen concentration in the culture medium. To obtain  
521 this expression, the limiting function of the Monod equation was reversed (Figure 9a).  
522 Figure 9b describes a function that equals zero for negligible dissolved oxygen  
523 concentration and increases suddenly with a vertical asymptote when dissolved oxygen  
524 concentration reaches the limit saturation ( $\tau S_{O_2}^{SAT}$ ). The parameter  $K_{PR}$ , based on the  
525 affinity constant of Monod switching functions, is responsible for the velocity at which  
526 the value of the function increases for increasing dissolved oxygen concentrations. The  
527 expression that describes the behaviour of photorespiration was obtained by subtracting  
528 a unit from the resulting function (Figure 9c).

529



530 Figure 9.a) Monod-function for limiting substrate, b) hyperbolic tangent function, c) photorespiration factor.

531  
 532  
 533 In an open reactor oxygen is gradually transferred from the culture medium to  
 534 the atmosphere, so the effect of photorespiration is negligible (as in our experiment).  
 535 Photorespiration should be considered in closed photobioreactors.

536 The calibrated value of the maximum specific growth rate of microalgae ( $\mu_{ALG} = 1.5 [d^{-1}]$ )  
 537 fits well within literature ranges  $[0.4-2 d^{-1}]$  (Reichert et al., 2001). Model results  
 538 proved to be very sensitive to mass transfer coefficients to the atmosphere (Table 4),  
 539 perhaps because all of these gases participate in a number of processes that either  
 540 promote or inhibit microalgae growth depending on their concentrations. Indeed, intense  
 541 photosynthesis can increase daytime dissolved oxygen levels in pond water up to more  
 542 than 200% of the saturation concentration (García et al., 2000b, Molina-Grima et al.,  
 543 2001). The exchange of dissolved oxygen between water and the atmosphere occurs  
 544 rapidly. Thus, to prevent high levels of dissolved oxygen in water, the coefficient of  
 545 volatilization of oxygen ( $K_{a,O_2}$ ) was set so that the oxygen concentration in the culture  
 546 medium would remain between 9 and 20  $g O_2 / m^3$ . Carbon dioxide and nitrogen mass  
 547 transfer were also calibrated. Although the values of these parameters can be found in  
 548 the literature as a function of surface interface, in this work we had to calibrate them  
 549 due to the 0D domain used.

550 In accordance with daily variation of light intensity, simulated curves show a  
 551 wavelike trend which indicates that model is able to reproduce the effects related to  
 552 microalgae processes occurring during daytime and at night.

## 553 8.2 Model limitations and future developments

554  
 555 In the current work a 0D domain was used to represent the microalgae culture in  
 556 the mesocosm. This approach was adequate for the specific characteristics of our  
 557 experimental system, since we assumed complete mixing conditions. However, HRAP  
 558 and photobioreactors are characterized by more complex geometries and hydrodynamic  
 559 regimes. In those cases both flow and transport equations will have to be coupled to the  
 560 current model to obtain realistic results.

561 Light attenuation caused by pigments absorption and by the scattering and the  
 562 shading effect of the microalgae cells themselves (Sutherland et al., 2014) was not

563 included in the current version of the model. However, numerous models (Quinn et al.,  
564 2011, Yuan et al. 2014) have been developed to estimate the gradient of light taking into  
565 account the aspects listed above.

566 Phosphorous species and their effects on biological processes were not included  
567 in this model since this component is usually highly available in wastewaters and hence  
568 it does not cause any growth-limiting effects on microalgae (Larsdotter, 2006).  
569 However, predictions on the rate of removal of phosphorous species will require their  
570 inclusion in the model, which in fact can be easily done following the approach of the  
571 RWQM1. Once all the above mentioned ameliorations are included in the model, it will  
572 be capable to predict biomass production in HRAP and photobioreactors. A following  
573 step to fulfil our final objective will be to complete the model with the addition of  
574 bacterial processes and to validate the model with other experimental data.

## 575 **8. Conclusions**

576 In this paper a complex biokinetic model to simulate the dynamics of microalgae  
577 growth is presented. The biokinetic model is based on RWQM1 formulation and was  
578 implemented in COMSOL Multiphysics<sup>TM</sup> together with several other processes  
579 affecting microalgal biomass production in the widest possible range of microalgal  
580 cultures.

581 The most relevant features of the model is the inclusion an allowance for carbon  
582 limitation on the growth of microalgae, as well as the dynamic model of photosynthesis  
583 and photolimitation and the description of the effect of photorespiration.

584 The model was calibrated by comparing simulated results to experimental data  
585 on microalgae growth in a mesocosm fed with synthetic culture medium (simulating a  
586 secondary effluent) for a period of 9 days. Although the results of the calibration indicate  
587 that the model was able to accurately reproduce microalgae growth, changes in nutrient  
588 concentrations and pH, the model will require a subsequent verification with other real  
589 dataset. The results of this paper have to be considered as a conceptual exercise that  
590 could be manually adjusted to fit one single experiment. The value of the exercise is in  
591 fact in the development of the equations set and showing that a model based on the set  
592 can be run and calibrated to fit a real dataset. Furthermore, the growth of microalgae  
593 under natural light/dark cycles and a dynamic model of  
594 photosynthesis (PSF) were implemented. The model was able to represent the complex  
595 system of photosynthetic growth with simultaneous photoinhibition and  
596 photorespiration.

597

598

599

## 600 **9. References**

601 Acien, F., Fernández Sevilla, J.M., Molina Grima, E. 2013. Photobioreactors for the production of microalgae.  
602 Reviews in Environmental Science and Bio/Technology, Volume 12, Issue 2, pp 131-151.

- 603 APHA-AWWA-WPCF (2001). APHA-AWWA-WPCF Standard Methods for the Examination of Water and  
604 Wastewater (twentieth ed.) American Public Health Association, Washington DC.
- 605 Al-Rawahi, N.Z., Zurigat, Y.H., Al-Azri N.A. 2011. Prediction of Hourly Solar Radiation on Horizontal and Inclined  
606 Surfaces for Muscat/Oma. The Journal of Engineering Research Vol 8 No 2, 19-31.
- 607 Avoz, Y., Goldman, J.C. 1982. Free ammonia inhibition of algal photosynthesis in intensive culture. Applied and  
608 Environmental Microbiology 43, 735-739.
- 609 Batstone, D., Keller, J., Angelidaki, R.I., Kalyuzhnyi, S.V., Pavlostathis, S.G., Rozzi, A., Sanders, W.T.M., Siegrist,  
610 H., Vavilin, V.A. (2002). Anaerobic Digestion Model No. 1 (ADM1). IWA Publishing, London.
- 611 Béchet, Q., Shilton, A., Guieysse, B., 2013. Modelling the effects of light and temperature on algae growth: State of  
612 the art and critical assessment for productivity prediction during outdoor cultivation. Biotechnology Advances 31,  
613 1648-1663.
- 614 Bernard, O., Masci, P., Sciandra, A. A photobioreactor model in nitrogen limited conditions. In: Proceedings of the  
615 sixth conference on mathematical modeling, Vienna, 2009.
- 616 Bitog, J.P., Lee, I.-B., Lee, C.-G., Kim, K.-S., Hwang, H.-S., Hong, S.-W., Seo, I.-H., Kwon, K.-S., Mostafa, E.  
617 2011. Application of computational fluid dynamics for modelling and designing photobioreactors for microalgae  
618 production: A review. Computers and Electronics in Agriculture 76(2), 131–147.
- 619 Bonachela, J.A., Raghieb, M., Levin, S.A. 2011. Dynamic model of flexible phytoplankton nutrient uptake. Proc. Natl.  
620 Acad. Sci. U.S.A. 108, 20633-20638.
- 621 Bouterfas, R., Belkoura, M., Dauta, A., 2002. Light and temperature effects on the growth rate of three freshwater  
622 [2pt] algae isolated from a eutrophic lake. Hydrobiologia 489, 207-217.
- 623 Brennan, L., Owende, P. Biofuels from microalgae—A review of technologies for production, processing, and  
624 extractions of biofuels and co-products. Renewable and Sustainable Energy Reviews, 14, Issue 2, 2010, 557-577.
- 625 Buhr, H.O., Miller, S.B. 1983. A dynamic model of the high-rate algal bacterial wastewater treatment pond. Water  
626 Res 17:29-37.
- 627 Camacho Rubio F, García Camacho F, Fernández Sevilla JM, Chisti Y, Molina Grima E., 2003. A mechanistic model  
628 of photosynthesis in microalgae. Biotechnol Bioeng;81(4): 459–73.
- 629 Camacho Rubio F., Ación Fernández F.G., García Camacho F., Sánchez Pérez J.A., Molina Grima E., 1999.  
630 Prediction of dissolved oxygen and carbon dioxide concentration profiles in tubular photo- bioreactors for microalgal  
631 culture. Biotechnology and bioengineering 62, 71–86.
- 632 Chisti, Y., 2007. Biodiesel from microalgae. Biotechnology advances 25(3), 294–306.
- 633 Craggs, R.J., Heubeck, S., Lundquist, T.J., Benemann, J.R. (2011). Algae biofuel from wastewater treatment high  
634 rate algal ponds. Water Sci. Technol. 63(4), 660-665.
- 635 Craggs, R., 2005. Advanced integrated wastewater pond. In: Shilton, A. (Ed.), Pond Treatment Technology, IWA  
636 Scientific and Technical Report Series, IWA, London, UK, pp. 282-310.
- 637 Crill, P.A., 1977. The photosynthesis-light curve: a simple analog model. J. Theor. Biol., 6: 506-516.
- 638 Dauta, A., Devaux, J., Piquemal, F., Boumnic, L. 1990. Growth rate of four freshwater algae in relation to light and  
639 temperatura. Hydrobiologia 207, 221-226.
- 640 Droop, M.R., 1968. Vitamin B<sub>12</sub> and marine ecology. IV. The kinetics of uptake, growth and inhibition in  
641 *Monochrysis lutheri*. J. Mar. Biol. Ass. U.K. 48, 689-733.
- 642 Droop, M.R., 1974. The nutrient status of algal cells in batch culture. J. Mar. Biol. Assoc. U.K. 54, 825-855.
- 643 Duffie J. and Beckman W., 1980. Solar Engineering of Thermal Processes.

- 644 Eilers, P.H.C., Peters, J.C.H., 1988. A model for the relationship between light intensity and the rate of  
645 photosynthesis in phytoplankton. *Ecological Modeling* 42, 199-215.
- 646 Franz, A., Lehr, F., Posten, C., Schaub, G., 2012. Modeling microalgae cultivation productivities in different  
647 geographic locations - estimation method for idealized photobioreactors. *Biotechnology Journal* 7(4), 546–557.
- 648 García, J., Hernández-Mariné, M., Mujeriego, R., 1998. Tratamiento de aguas residuales urbanas mediante lagunas de  
649 alta carga: evaluación experimental. *Tratamiento de Aguas Residuales Urbanas* 5, 35–50.
- 650 García, J., Hernández-Mariné, M., Mujeriego, R., 2008b. High rate algal pond operating strategies for urban  
651 wastewater nitrogen removal. *Journal of Applied Phycology* 12, 331-339.
- 652 Guisasola, A., Petzet, S., Baeza, J., Carrera, J., Lafuente, J., 2007. Inorganic carbon limitations on nitrification :  
653 Experimental assessment and modelling. *Water research* 41, 277–286.
- 654 Harris, G.P. 1978. Photosynthesis, productivity and growth: the physiological ecology of phytoplankton. *Ergebnisse  
655 der limnologie* 10, 1-171.
- 656 Henze, M., Gujer, W., Mino, T., van Loosdrecht, M., 2000. Activated sludge models ASM1, ASM2, ASM2d and  
657 ASM3. IWA Scientific and Technical Report No. 9, IWA Publishing, London, UK.
- 658 Huisman, J. Population dynamics of light-limited phytoplankton: microcosm experiments. *Ecology* 1999; 80 202–10.
- 659 Khorsandi, H., Alizadeh, R., Tosinejad, h., Porghaffar, H. 2014. Analysis of nitrogenous and algal oxygen demand in  
660 effluent from a system of aerated lagoons followed by polishing pond. *Water Science & Technology* 70.1 – 95.
- 661 Kong, Q.X., Li, L., Martinez, B., Chen, P., Ruan, R., (2010). Culture of microalgae *Chlamydomonas reinhardtii* in  
662 wastewater for biomass feedstock production. *Applied biochem. and Biotechnol.* 160, 9–18.
- 663 Kurano, N., Miyachi, S., 2005. Selection of microalgal growth model for describing specific growth rate-light  
664 response using extended information criterion. *Journal of Bioscience and Bioengineering* 100(4), 403–408.
- 665 Langergraber, G., Rousseau, D., García, J., Mena, J., 2009. CWM1: a general model to describe biokinetic processes  
666 in subsurface flow constructed wetlands. *Water science and technology : a journal of the International Association on  
667 Water Pollution Research* 59(9), 1687–97.
- 668 Larsdotter, K., 2006. Wastewater treatment with microalgae-a literature review. *Vatten*, 31–38.
- 669 Liu, B., Jordan, R. 1960. The interrelationship and characteristic distribution of direct, diffuse and total solar radiation.  
670 *Solar Energy*, Volume 4, Issue 3, July 1960, Pages 1-19
- 671 Luo, H.-P., Al-Dahhan, M.H., 2004. Analyzing and modeling of photobioreactors by combining first principles of  
672 physiology and hydrodynamics. *Biotechnology and bioengineering* 85(4), 382–93.
- 673 Molina Grima, E., AcienFernández, G., Chisti, Y., 1999. Photobioreactors: light regime, mass transfer, and scaleup.  
674 *Journal of biotechnology* 70, 231–247.
- 675 Molina Grima, E., Fernández, J., AcienFernández, G., Chisti, Y., 2001. Tubular photobioreactor design for algae  
676 cultures. *Journal of biotechnology* 92, 113–131.
- 677 Monod, J., 1949. The growth of bacterial cultures. *Annual Reviews in Microbiology* 3, 371-394.
- 678 Morris, M.D. 1991. Factorial Sampling Plans for Preliminary Computational Experiments. *Technometrics*, Vol. 33,  
679 No. 2. pp. 161-174.
- 680 Mostert, E.S., Grobbelaar, J.H. 1987. The Influence of Nitrogen and Phosphorus on Algal Growth and Quality in  
681 Outdoor Mass Algal Cultures. *Biomass* 13 (1987) 219-233.
- 682 Novak, J.T., Brune, D.E. 1985. Inorganic carbon limited growth kinetics of some freshwater algae. *Water Res.* 19,  
683 215-225.

684 Oswald, W.J. (1998a). Micro-algae and waste-water treatment. In Borowitzka MA, Borowitzka LJ. (eds) Micro-algal  
685 Biotechnology. Cambridge U.P., Cambridge, 305-328.

686 Packer A, Li Y, Andersen T, Hu Q, Kuang Y, Sommerfeld M. Growth and neutral lipid synthesis in green  
687 microalgae: a mathematical model. *BioresourTechnol* 2011;102:111–7.

688 Park, J. B. K., Craggs, R. J. 2011. Algal production in wastewater treatment high rate algal ponds for potential biofuel  
689 use. *Water Sci. Technol.*, 63(10), 2403-2410.

690 Park, J.B.K., Craggs, R.J., Shilton, A.N., 2011a. Wastewater treatment high rate algal ponds for biofuel  
691 production. *Bioresource Technology*, 102(1), 35–42.

692 Quinn, J., de Winter, L., Bradley, T., 2011. Microalgae bulk growth model with application to industrial scale  
693 systems. *Biosource Technology* 102, 5083-5092.

694 Reichert, P., Borchardt, D., Henze, M., Rauch, W., Shanahan, P., Somlyódy, L., Vanrolleghem, P., 2001. River Water  
695 Quality Model no. 1 (RWQM1): II. Biochemical process equations. *Water science and technology : a journal of the*  
696 *International Association on Water Pollution Research* 43(5), 11–30.

697 Sah, L., Rousseau, D., Hooijmans, C.M., Lens, P., 2011. 3D model for a secondary facultative pond. *Ecological*  
698 *Modelling* 222(9), 1592–1603.

699 Sah, L., Rousseau, D., Hooijmans, C.M., 2012. Numerical Modelling of Waste Stabilization Ponds: Where Do We  
700 Stand? *Water, Air, & Soil Pollution* 223(6), 3155-3171.

701 Syrett, P.J. 1981. Nitrogen metabolism of microalgae. In *Physiological bases of phytoplankton ecology* (T. Platt, ed.).  
702 *Canadian Bulletin of Fisheries and Aquatic Sciences* 210:182-210.

703 Silva, H.J., Pirt, J. 1984. Carbon dioxide inhibition of photosynthetic growth of chlorella. *Journal of General*  
704 *Microbiology*, 130, 2833-2838.

705 Sperling, M. V. 2007. *Waste stabilization ponds*. IWA Publishing, London, Uk.

706 Spolaore, P., Joannis-Cassan, C., Duran, E., Isambert, A. Commercial Applications of Microalgae. *Journal of*  
707 *bioscience and bioengineering* 2006, 101, 87–96.

708 Stewart, W. D. P. (1974). *Algal physiology and biochemistry*, Blackwell Scientific Publications, Oxford, 989 pp.

709 Talbot, P., Gortares, M.P., Lencki, R.W., Noue de la J (1991). Absorption of CO<sub>2</sub> in algal mass culture systems: A  
710 different characterization approach. *BiotechnolBioeng* 37:834-842.

711 Wu, X., Merchuk, J., 2001. A model integrating fluid dynamics in photosynthesis and photoinhibition processes.  
712 *Chemical Engineering Science* 56, 3527–3538.

713 Yuan, S., Zhou, X., Chen, R., Song, B., 2014. Study on modelling microalgae growth in nitrogen-limited culture  
714 system for estimating biomass productivity. *Renewable and Sustainable Energy Reviews* 34 525-535.

715 Zonneveld, C., 1998. Light-limited microalgae growth: a comparison of modelling approaches. *Ecological Modelling*  
716 113 41-54.

717

718

## Supplementary Tables

Supplementary Table 1. Values of biokinetic and physic parameters.

Parameters	Description	Value	Unit	Source
<b>Microalgae processes</b>				
$\mu_{ALG}$	Maximum growth rate of microalgae	1,6	$d^{-1}$	Calibrated
$k_{resp,ALG}$	Endogenous respiration constant	0,1	$d^{-1}$	(Reichert et al., 2001)
$k_{death,ALG}$	Inactivation constant	0,1	$d^{-1}$	(Reichert et al., 2001)
$K_{C,ALG}$	Affinity constant of microalgae on carbon species	0,00432	$gC/m^3$	(Novak and Brune, 1985)
$I_{CO2,ALG}$	$CO_2$ inhibition constant of microalgae	120	$gC/m^3$	(Silva and Pirt, 1984)
$K_{N,ALG}$	Affinity constant of microalgae on nitrogen species	0,1	$gN/m^3$	(Reichert et al., 2001)
$K_{O2,ALG}$	Affinity constant of microalgae on dissolvedoxygen	0,2	$gO_2/m^3$	(Reichert et al., 2001)
<b>Photorespiration factor</b>				
$K_{PR}$	Inhibition constant of photorespiration	0,01	–	Assumption
$\tau$	Coefficient of excess dissolved oxygen	4	–	(Chisti, 2007)
$S_{O2}^{SAT}$	Saturation concentration of oxygen in the air	7,1904	$gO_2/m^3$	(Camacho Rubio et al., 1999)
<b>Photosynthetic thermal factor</b>				
$T_{OPT}$	Optimum temperature for microalgae growth	25	$^{\circ}C$	(Dauta et al., 1990)
s	Normalized parameter	13	–	(Dauta et al., 1990)
<b>Light factor</b>				
$\alpha$	Parameter activation	0,001935	$(\mu E/m^2)^{-1}$	(Wu andMerchuk, 2001)
$\beta$	Parameter inhibition	$5,7848 * 10^{-7}$	$(\mu E/m^2)^{-1}$	(Wu and Merchuk, 2001)
$\gamma$	Parameter production	0,1460	$s^{-1}$	(Wu and Merchuk, 2001)
$\delta$	Parameter recovery	0,0004796	$s^{-1}$	(Wu and Merchuk, 2001)
<b>Irradiance solar incident</b>				
$E_f$	Photosynthetic efficiency of solar radiation	1,74	$\mu E/J$	(Molina Grima et al., 1999)
$\aleph$	Index atmospheric clarity	0,74	–	(Molina Grima et al., 1999)
$\zeta$	Universal solar constant	1353	$W/m^2$	(Molina Grima et al. 1999)
$\omega$	Hour angle	Calculated	$^{\circ}$	(Liu and Jordan, 1960)
$\omega_s$	Sunset hour angle	Calculated	$^{\circ}$	(Liu and Jordan, 1960)
$\varphi$	Latitude	Observed	$^{\circ}$	-
$\delta$	Sun declination	Calculated	$^{\circ}$	(Liu and Jordan, 1960)
<b>Transferof gasesto the atmosphere</b>				
$K_{a,O2}$	Mass transfer coefficient for oxygen	4	$d^{-1}$	Calibrated
$K_{a,CO2}$	Mass transfer coefficient for dioxide carbon	0.7	$d^{-1}$	Calibrated
$K_{a,NH3}$	Mass transfer coefficient for ammonia	0.7	$d^{-1}$	Calibrated

Supplementary Table 2. Values of chemical parameters.

Parameters	Equations
Chemical equilibrium $CO_2 \leftrightarrow HCO_3^-$ .	$K_{eq,1} = 10^{17,843 - \frac{3404,71}{273,15+T} - 0,032786(273,15+T)}$

Chemical equilibrium $\text{HCO}_3^- \leftrightarrow \text{CO}_3^{2-}$	$K_{\text{eq},2} = 10^{9,494 \frac{2902,39}{273,15+T} - 0,02379(273,15+T)}$			
Chemical equilibrium $\text{NH}_4^+ \leftrightarrow \text{NH}_3$	$K_{\text{eq},3} = 10^{2,891 - 2727/(273,15+T)}$			
Chemical equilibrium $\text{H}^+ \leftrightarrow \text{OH}^-$	$K_{\text{eq},w} = 10^{-\frac{4470,99}{273,15+T} + 12,0875 - 0,01706(273,15+T)}$			
<b>Kinetics parameters</b>				
$k_{\text{eq},1}$	Dissociation constant of $\text{CO}_2 \leftrightarrow \text{HCO}_3^-$	10000	$\text{d}^{-1}$	(Reichert et al., 2001)
$k_{\text{eq},2}$	Dissociation constant of $\text{HCO}_3^- \leftrightarrow \text{CO}_3^{2-}$	1000	$\text{d}^{-1}$	(Reichert et al., 2001)
$k_{\text{eq},3}$	Dissociation constant of $\text{NH}_4^+ \leftrightarrow \text{NH}_3$	1000	$\text{d}^{-1}$	(Reichert et al., 2001)
$k_{\text{eq},w}$	Dissociation constant of $\text{H}^+ \leftrightarrow \text{OH}^-$	1000	$\text{g}^*\text{m}^{-1}*\text{d}^{-1}$	(Reichert et al., 2001)

Supplementary Table 3. Mathematical expressions of the stoichiometric coefficients of each process.

Stoichiometric coefficient	Unit
<b>Microalgae growth on ammonia</b>	
$v_{1,1a} = -i_{\text{N,ALG}}$	gN/gCOD
$v_{4,1a} = \frac{8i_{\text{C,ALG}}}{3} + 8i_{\text{H,ALG}} - i_{\text{O,ALG}} - \frac{12i_{\text{N,ALG}}}{7}$	gO <sub>2</sub> /gCOD
$v_{5,1a} = -i_{\text{C,ALG}}$	gC/gCOD
$v_{8,1a} = \frac{i_{\text{N,ALG}}}{14}$	gH/gCOD
$v_{10,1a} = 1$	gCOD/gCOD
<b>Microalgae growth on nitrate</b>	
$v_{3,1b} = -i_{\text{N,ALG}}$	gN/gCOD
$v_{4,1b} = \frac{8i_{\text{C,ALG}}}{3} + 8i_{\text{H,ALG}} - i_{\text{O,ALG}} - \frac{20i_{\text{N,ALG}}}{7}$	gO <sub>2</sub> /gCOD
$v_{5,1b} = -i_{\text{C,ALG}}$	gC/gCOD
$v_{8,1b} = -\frac{i_{\text{N,ALG}}}{14}$	gH/gCOD
$v_{10,1b} = 1$	gCOD/gCOD
<b>Microalgae endogenous respiration</b>	
$v_{1,2} = i_{\text{N,ALG}}$	gN/gCOD
$v_{4,2} = (i_{\text{O,ALG}}) - 8(i_{\text{H,ALG}}) - \frac{8}{3}(i_{\text{C,ALG}}) + \frac{12}{7}(i_{\text{N,ALG}})$	gO <sub>2</sub> /gCOD
$v_{5,2} = i_{\text{C,ALG}}$	gC/gCOD
$v_{8,2} = -\frac{1}{14}(i_{\text{N,ALG}})$	gH/gCOD
$v_{10,2} = -1$	gCOD/gCOD
<b>Microalgae inactivation</b>	
$v_{1,3} = i_{\text{N,ALG}}$	gN/gCOD
$v_{4,3} = (i_{\text{O,ALG}}) - 8(i_{\text{H,ALG}}) - \frac{8}{3}(i_{\text{C,ALG}}) + \frac{12}{7}(i_{\text{N,ALG}})$	gO <sub>2</sub> /gCOD
$v_{5,3} = i_{\text{C,ALG}}$	gC/gCOD
$v_{8,3} = -\frac{1}{14}(i_{\text{N,ALG}})$	gH/gCOD
$v_{10,3} = -1$	gCOD/gCOD
<b>Chemical equilibria <math>\text{CO}_2 \leftrightarrow \text{HCO}_3^-</math></b>	
$v_{5,4} = -1$	gC/gC
$v_{6,4} = 1$	gC/gC
$v_{8,4} = 1/12$	gH/gC
<b>Chemical equilibria <math>\text{HCO}_3^- \leftrightarrow \text{CO}_3^{2-}</math></b>	
$v_{6,5} = -1$	gC/gC
$v_{7,5} = 1$	gC/gC
$v_{8,5} = 1/12$	gH/gC
<b>Chemical equilibria <math>\text{NH}_4^+ \leftrightarrow \text{NH}_3</math></b>	

$v_{1,6} = -1$	gN/gN
$v_{2,6} = 1$	gN/gN
$v_{8,6} = 1/14$	gH/gN
<b>Chemical equilibria <math>H^+ \leftrightarrow OH^-</math></b>	
$v_{8,7} = 1$	gH/gH
$v_{9,7} = 1$	gH/gH
<b>Oxygen transfer to the atmosphere</b>	
$v_{4,O_2} = 1$	–
<b>Carbon dioxide transfer to the atmosphere</b>	
$v_{5,CO_2} = 1$	–
<b>Ammonia transfer to the atmosphere</b>	
$v_{2,NH_3} = 1$	–

Supplementary Table 4. Values of fraction of carbon, hydrogen, oxygen and nitrogen in microalgae biomass.

Parameter	Description	Value	Unit	Source
<b>Fractions of microalgal biomass</b>				
$i_{C,ALG}$	Fraction of carbon in microalgae	0,387	gC/gCOD	(Reichert et al., 2001)
$i_{H,ALG}$	Fraction of hydrogen in microalgae	0,075	gH/gCOD	(Reichert et al., 2001)
$i_{O,ALG}$	Fraction of oxygen in microalgae	0,538	gO/gCOD	(Reichert et al., 2001)
$i_{N,ALG}$	Fraction of nitrogen in microalgae	0,065	gN/gCOD	(Reichert et al., 2001)